A Novel Hybrid Control for Maximizing Power in a Photovoltaic System

Iyad Ameur[1], Mohammed Benmiloud[2], Atallah Benalia[1]

[1]LACoSERE laboratory, Electrical Engineering Department, Amar Telidji University, 03000 Laghouat, Algeria

[2]Department of Engineering, University of Cambridge, United Kingdom

Abstract

This article is devoted to the development of a hybrid algorithm to track the maximum power in a photovoltaic system using a multicellular converter. The requirements of Maximum Power Point Tracking (MPPT) can be summarized in a fast transient and a minimal oscillation at the maximum power point (MPP). This can be met in two steps by using the hybrid systems theory: i) a hybrid transient automaton, that ensures a fast convergence by a minimal settling time and low number of commutations, and ii) a hybrid steady-state automaton that guarantees the minimum stress around the MPP. To justify a hybrid MPPT as a viable MPPT option, a comprehensive comparison is carried out between the proposed MPPT and the two methods; the Perturb and Observe (P & O) and the Incremental Conductance (IC). The results show that the hybrid MPPT is capable of tracking the MPP with higher performance under various types of environmental changes.

Keywords: Photovoltaic system, Maximum power point tracking-MPPT, multicellular converter, hybrid dynamical theory

Received: 01 April 2019

To cite this article:
Ameur I., Benmiloud M., Benalia A., "A Novel Hybrid Control for Maximizing Power in a Photovoltaic System", in *Electrotehnica, Electronica, Automatica (EEA)*, 2019, vol. 67, no. 3, pp. 05-13, ISSN 1582-5175.

1. Introduction

The rapid development of industries and the growing population are putting global energy supplies under enormous pressure. Furthermore, the climate change issue and the need to reduce carbon have prompted companies and nations to invest in alternative energy sources, particularly the renewable energy. Solar Photovoltaic (PV) is one of the most important sources of renewable energy. This is due to many factors including the abundant source, the easiness of installing, almost free maintenance, and most importantly it is environmentally friendly [1, 2].

Although these advantages, photovoltaic systems have not achieved parity with fossil-based networks, which is due to the low efficiency with high cost of photovoltaic units. It is important to enhance the energy production of the PV system by improving the ability to track the maximum power point (MPP) during the continuous change in the environmental situation such as temperature and solar radiation [3]. Each photovoltaic (PV) generator is characterized by the P-V curve, which is nonlinear and have one global maximum power point.

To guarantee that the maximum power from the PV array be always achieved, we need to employ adaptation stages like a DC-DC converter in order to maximize the PV production by coinciding the operating point with the maximum power point MPP in the P-V curve [4, 5, 6].

Many topologies have been proposed as an adaptation device between the PV array and the DC bus. They have to meet certain practical challenges such as reliability, high power density, high efficiency and low ripple current/voltage. Conventional converters do not meet the above requirements with better scaling power characteristics. Multicellular parallel converters are a good alternative to conventional ones. For the case of the conventional buck converter, there is the analogous N-interleaved-buck converter, which is composed of N cells of conventional buck converters.

The interleaved topologies are widely used in renewables such as solar panels and fuel cells [7]. The main objective of this topology is to reduce the ripple of the input current, support high input current and reduce the constraints on the power components [8, 9]. Some research studies discussed the interleaving technique from the point of view the number of cells (also called phases) and their impact on inductor volume, switching losses, and the input current ripples [10].

Other research focused on its control problem, the aim of the control in a photovoltaic system is generally to extract the maximum energy from the

solar panel, such control schemes are known in the literature with Maximum Power point Tracking (MPPT) algorithms [11, 12, 13].

Many algorithms are published in order to improve the performance of the MPPT, in matter of speed and quantity of production. These algorithms can be classified into two categories; Traditional algorithms, and soft computing algorithms [1, 2]. In the class of traditional methods, there is the very popular "Perturb and Observe (P&O)" algorithm [9, 14, 15], Incremental Conductance (InCond) [16, 17], and Hill Climbing (HC) [18]. Besides, there is uncommon methods like the fractional short circuit current, the fractional open circuit voltage, and the ripple correlation control [19, 20].

This category has good advantages in terms of tracking efficiency, and convergence speed, it experiences however the very serious defect of the continuous fluctuation around the steady state, which results in a significant power loss. In addition, none of these algorithms can handle with a situation of non-uniform radiation.

In class of soft computing methods, a variety of algorithms based on FL: Fuzzy Logic, ANN: Artificial Neural Network, GA: Genetic Algorithms, ACO: Ant Colony Optimization, PSO: Particle Swarm Optimization [21, 22, 23, 24, 25]. This category has good advantages, the most important of which is accuracy and flexibility, but its disadvantages are shocking. It inherits complexity and slowness (essentially in ANN), and this leads to the need of a special microprocessor that is expensive. Motivated by the above facts, we aim to alleviate some of these problems.

This paper proposes a new MPPT technique in the framework of hybrid automata theory. The proposed algorithm is given as guard conditions, which govern the switching between the different converter modes. The converter investigated in our approach is a two-cell converter, this choice is justified by the reduced input current ripple offered by the two-cell converter over the conventional buck (one-cell) converter, and this leads the MPPT to operate around a maximum power point without too much fluctuation. For this purpose, an instantaneous model of the converter will be investigated in the next section in the framework of hybrid dynamical systems theory.

The paper is organized as follows: In section 2, a mathematical model of the PV system is illustrated. Section 3 presents the hybrid (switched) dynamical model of the converter using hybrid systems theory. In section 4, a detailed synthesis on the proposed Hybrid MPPT is given as discrete modes and guard conditions. Then, Section 5 discusses simulation results under different working conditions. The two performance tests with the standard MPPT algorithms are also provided. Finally, a conclusion will summarize and discuss the obtained results.

2. Hybrid Model of two Interleaved Buck Converter

The interleaved buck converter is based on the association of K phases, each phase consists of an inductor ($\boldsymbol{L_k}$), a diode ($\boldsymbol{D_k}$), and a semiconductor device ($\boldsymbol{sw_k}$). The control switches are represented by a binary input signal $\boldsymbol{u_k \epsilon \{0, 1\}}$, where the values 0 and 1 stand for the states "blocking" and "conducting", respectively. The phase number increase leads to very accurate results, but on the other hand, the complexity of the system increases.

In the present paper, we consider the two-phase case.

Figure 1 represents the two-interleaved buck converter (2IBC) feeding a resistive load (R) and operating in continuous conduction mode (CCM).

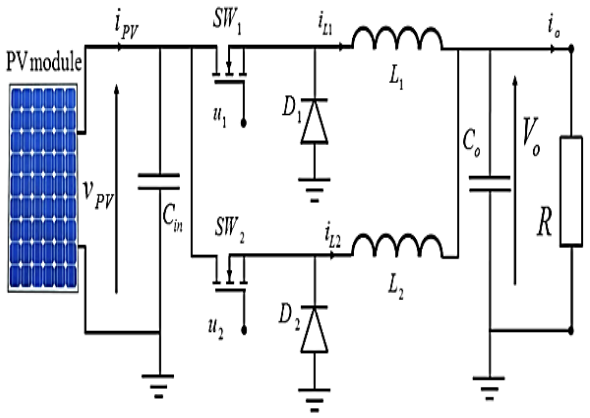

Figure 1. Structure of the photovoltaic module with 2-phase interleaved buck converter (PV-2IBC)

Therefore, the dynamics of the PV array with the (2IBC) are given by:

$$\begin{cases} \frac{di_{L_k}}{dt} = \frac{v_{in}u_k - v_o}{L_k} \\ \frac{dv_o}{dt} = \frac{1}{c_o}\left(\sum_{k=1}^{2} i_{L_k} - \frac{v_o}{R}\right) \\ \frac{dv_{pv}}{dt} = \frac{1}{c_{in}}\left(i_{pv} - \sum_{k=1}^{2} u_k\, i_{L_k}\right) \end{cases} , K = 1,2 \qquad (1)$$

where i_{L_k} is the inductor current of phase k, v_{pv} is the input voltage, v_o is the output.

The input signals (u_1; u_2) combinations offer four different modes of operation, these modes take the name "discrete modes" in the framework of hybrid systems. System (1) can be written in the following switched affine form:

$$\dot{x} = A_{q_i}x + B_{q_i} = f_{q_i}(x) \qquad (2)$$

where: $x = [\, i_{L_1} \quad i_{L_2} \quad v_{pv} \quad v_o \,]^T \in X$ is the continuous state vector defined in a physical operating region $X \subseteq \mathbb{R}^4$; q(t) : $\mathbb{R}_+ \longrightarrow Q$ is the switching signal that takes its values in a finite set of discrete modes $Q = \{q_1; q_2; q_3; q_4\}$.

The state matrices $A_{q_i} \in \mathbb{R}^{4\times4}$ and $B_{q_i} \in \mathbb{R}^{4\times1}$ are given by:

$$A_{q_i} = \begin{pmatrix} 0 & 0 & \frac{u_1}{L_2} & \frac{-1}{L_1} \\ 0 & 0 & \frac{u_2}{L_2} & \frac{-1}{L_2} \\ \frac{-u_1}{c_{in}} & \frac{-u_2}{c_{in}} & \frac{u_2}{L_2} & 0 \\ \frac{-u_1}{c_o} & \frac{-u_1}{c_o} & 0 & \frac{-1}{R} \end{pmatrix} B_{q_i} = \begin{pmatrix} 0 \\ 0 \\ \frac{i_{pv}}{c_{in}} \\ 0 \end{pmatrix}$$

In the remainder of the paper, we will consider $L_1 = L_2 = L$.

Hybrid systems can be defined as dynamical systems whose behaviour is determined by the interaction of continuous and discrete dynamics [26-28].

In the modelling and analysis of such systems, we need the combination of continuous dynamics described by differential equations with discrete events described by an automata or Petri nets [29].

One can remark from the structure of the system in Figure 1 that the coexistence of continuous variables (capacitor voltages v_{in}, v_o, and inductor currents i_{L_1}, i_{L_2}) and discrete variables (states of the switches) present a hybrid behavior. This justifies the use of hybrid modeling for the analysis and control design of the PV system. In this study, the hybrid automaton, which is formulated by the following 6-tuple, can represent the PV system.

$$H = (Q, X, S_c, T, G, I_{nit}) \quad (3)$$

where $Q = \{q_i; i \in 1, \dots, 4\}$ is a set of four discrete modes.

Each one corresponds to a specific topology of the converter obtained by the states of the switches (see Table 1).

$$X = \left\{x \in \mathbb{R}^4 / 0 \le i_{L_k} \le i_{L_{kmax}} \wedge 0 \le v_{pv} \le v_{oc} \wedge 0 \le v_o \le v_{max}\right\}, k = 1,2$$

is the continuous state space that characterizes the operating states of the converter, with

$$x = [\, i_{L_1} \quad i_{L_2} \quad v_{pv} \quad v_o \,]^T \in X \text{ and } i_{L_{kmax}}$$

is the maximum current that can be delivered by the phase k.

$S_c : (Q \times X) \longrightarrow \mathbb{R}^4$ is the application that assigns to every discrete mode a continuous dynamic given by (2).

$$T = \left\{T_{ij}, i, j \in \{1, \dots, 4\}\right\}$$

represents a set of all possible transitions between discrete modes.

G: $T \longrightarrow 2^x$ associates to each transition a continuous set where the transition is valid (called a guard condition). $I_{nit} \subseteq \mathrm{X} \times Q$ is the set of initial states [29].

In the hybrid modelling of the photovoltaic array, two discrete modes can be distinguished q_{pv1}, q_{pv2}, the first increases the voltage v_{pv} while the second decreases this voltage. We can classify the four discrete modes of the 2IBC into two classes, the first class leads to increase the voltage v_{pv} this means activating the mode q_{pv1}, and the other class leads to decrease the voltage v_{pv}, this means activating the mode q_{pv2}.

Table 1. The discrete modes of the PV system with the two interleaved buck converter

Discrete modes		Inputs		Currents evolution		voltage evolution
PV array	Buck converter	u_1	u_2	i_{L_1}	i_{L_2}	v_{pv}
$\boldsymbol{q_{pv1}}$	q_1	0	0	↘	↘	↗
$\boldsymbol{q_{pv2}}$	q_2	1	0	↗	↘	↘
	q_3	0	1	↘	↗	↘
	q_4	1	1	↗	↗	↘

In Table 1, we summarized these discrete modes and the evolution of the system variables. In the input current, the up arrow means that the inductor is charging, while that the down arrow means that the inductor is discharging.

In the input voltage v_{pv}, the up and the down arrow means the increase and decrease in the voltage of the PV array respectively, all is based on the switching design. In the next subsection, we will solve the MPP problem.

3. Control Design: Hybrid MPPT

The problem of the control design of the PV system is to the maximization of the PV energy production with a minimum switching among the discrete modes $Q = \{q_1; q_2; q_3; q_4\}$ and a fast transient property. This problem is not directly discussed using the theory of continuous dynamic systems.

In this section, we will solve this problem efficiently using the theory of hybrid systems. We can reformulate this problem as follows:

(1) How one should select the convenient discrete modes among the set Q in order to fast reach a neighbourhood of the MPP, with the fast balance of the input current between the two phases;

(2) When a neighbourhood of the MPP is reached, how to select the discrete modes to ensure that the operating point is coincident with the maximum power point.

It should be noted that the hybrid control of the 2IBC is done with the purpose of tracking the MPP without need of a Pulse Width Modulation (PWM) control to generate the switching signals.

Moreover, we can design an algorithm in two parts as shown in Figure 2, a transient state automaton for fast convergence to the MPP and a steady state automaton to maintain the system operating point in the maximum power point.

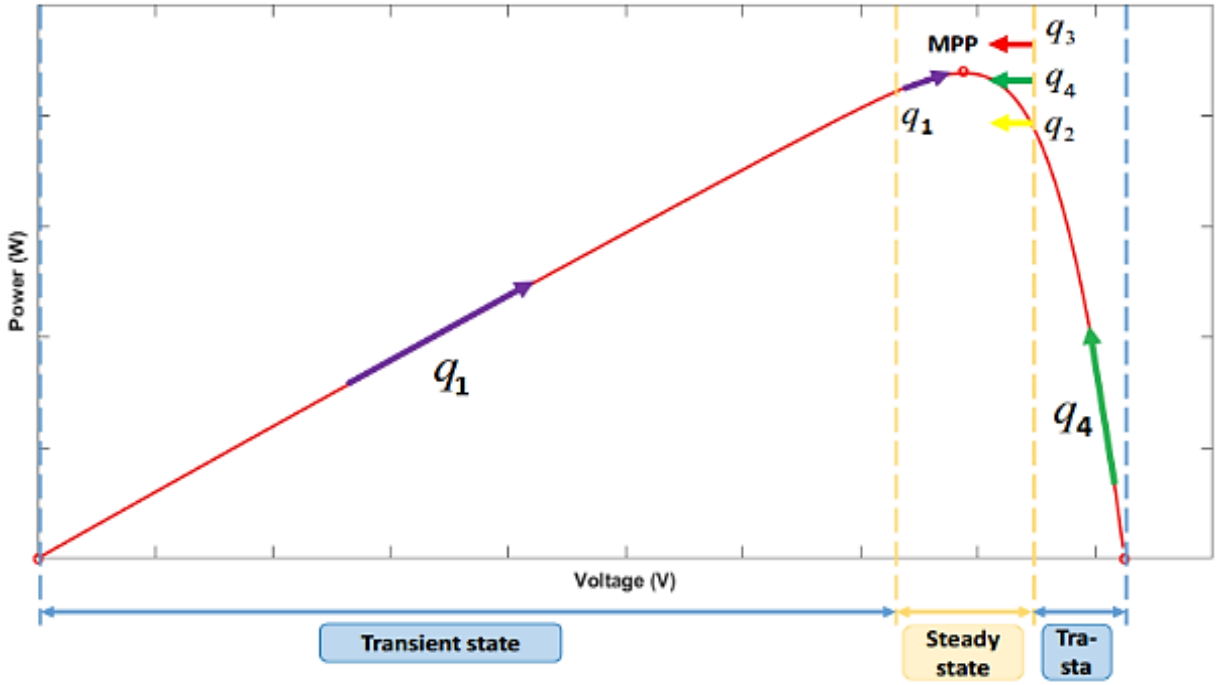

Figure 2. Evolution of the MPP tracking in the P-V curve

3.1 Transient Automaton Design

According to the characteristics of the PV array (P-V curve), we can assert that there exists only one voltage value for which the PV arrays deliver the maximum power as shown in Figure 2.

In order to achieve the fast convergence of the PV voltage to a neighboured of V_{mpp}, one can distinguish two cases:

- If the operating point is on the left side of the MPP, meaning that $v_{pv} < v_{mpp}$: The selected discrete mode in this region must ensure an increasing value of the PV voltage v_{pv}. From the voltage evolution in Table 1, it can be observed that mode q_1 is the only appropriate option in this region; we apply this mode in order to force the operating point to fast reach the MPP as illustrated in Figure 2.

If the operating point is on the right side of the MPP, meaning that $v_{pv} > V_{mpp}$: One should select the discrete mode that guarantees a decreasing value of the PV voltage to fast reach the V_{mpp}. From Table 1, one of the modes $q_2; q_3; q_4$ is appropriate for this situation in order to compel the operating point to access the MPP as shown in Figure 2.

Figure 3 shows the proposed hybrid automaton of the 2IBC with both transient and steady control parts, where each node represents a discrete mode and the arrows indicate the possible discrete transitions.

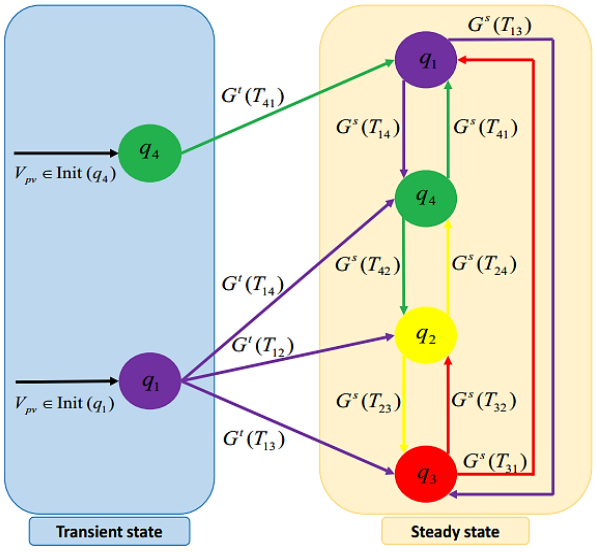

Figure 3. The proposed hybrid automaton of the photovoltaic system (PV-2IBC)

We can say that the PV voltage of the PV array reached the desired value V_{mpp} in finite time and within only one commutation (q_1 or q_4). The transient automaton controller corresponds to the above analysis where the elements (G; T; I_{nit}) are defined as follows:

- The initial discrete mode depends on the initial continuous state (input voltage v_{pv}) as follows:

$$I_{nit} = (I_{nit}(q_1) \times q_1) \cup (I_{nit}(q_2) \times q_2) \cup (I_{nit}(q_3) \times q_3) \cup (I_{nit}(q_4) \times q_4) \quad (4)$$

with

$$I_{nit}(q_1) = \{x \in \mathbb{R}/\ v_{pv} < v_{mpp}\},\ I_{nit}(q_2) = \{x \in \mathbb{R}/\ (v_{pv} > v_{mpp}) \wedge (i_{L_1} > i_{L_2})\}$$

$$I_{nit}(q_4) = \{x \in \mathbb{R}/\ v_{pv} > v_{mpp}\},\ I_{nit}(q_3) = \{x \in \mathbb{R}/\ (v_{pv} > v_{mpp}) \wedge (i_{L_1} < i_{L_2})\}$$

- The guard conditions corresponding to the transition to the steady-state automaton are given by:

$$G^t(T_{41}) = \left\{x \in \frac{\mathrm{x}}{v_{pv}<v_{mpp}}\right\}$$

$$G^t(T_{14}) = \left\{x \in \frac{\mathrm{X}}{v_{pv} > v_{mpp}} \wedge \left(i_{L_1} = i_{L_2}\right)\right\}$$

$$G^t(T_{12}) = \left\{x \in \frac{\mathrm{x}}{v_{pv}>v_{mpp}} \wedge \left(i_{L_1} < i_{L_2}\right)\right\} \quad (5)$$

$$G^t(T_{13}) = \left\{x \in \frac{\mathrm{X}}{v_{pv} > v_{mpp}} \wedge \left(i_{L_2} > i_{L_1}\right)\right\}$$

3.2 Steady-State Automaton Design

Once the operating point reaches the maximum power point, a steady-state automaton must be activated to guarantee the local stability of the desired value (v_{mpp}). For this purpose, the algorithm switches between the different modes of the 2-IBC using an automaton governed by the currents (i_{L_1}, i_{L_2}) and the status of power.

The voltage oscillates in the neighbourhood of v_{mpp}. A small range of oscillation causes a small loss of power, which means better control, and vice versa, we can achieve that by the low ripple in the input current and it is the main feature of the proposed converter (2-IBC).

Figure 3 illustrates the operation of the steady-state automaton, located near the MPP. In this case, we use two discrete modes: q_1, if the operating point is in the left side of the MPP, and one of the rest modes (q_2, q_3 or q_4), depending on the situation, if the operating point is on the right side of the MPP. The guard conditions corresponding to the steady-state automaton are defined as follows:

$$G^s(T_{41}) = \left\{x \in \frac{\mathrm{x}}{v_{pv}<v_{mpp}} \wedge \left(i_{L_1} = i_{L_2}\right)\right\}$$

$$G^s(T_{14}) = \left\{x \in \frac{\mathrm{X}}{v_{pv} > v_{mpp}} \wedge \left(i_{L_1} = i_{L_2}\right)\right\}$$

$$G^s(T_{24}) = \left\{x \in \frac{\mathrm{X}}{v_{pv} > v_{mpp}} \wedge \left(i_{L_1} = i_{L_2}\right)\right\}$$

$$G^s(T_{42}) = \left\{x \in \frac{\mathrm{X}}{v_{pv} > v_{mpp}} \wedge \left(i_{L_2} < i_{L_1}\right)\right\}$$

$$G^s(T_{23}) = \left\{x \in \frac{\mathrm{x}}{v_{pv}>v_{mpp}} \wedge \left(i_{L_2} > i_{L_1}\right)\right\} \quad (6)$$

$$G^s(T_{32}) = \left\{x \in \frac{\mathrm{X}}{v_{pv} > v_{mpp}} \wedge \left(i_{L_2} < i_{L_1}\right)\right\}$$

$$G^s(T_{12}) = \left\{x \in \frac{\mathrm{x}}{v_{pv}>v_{mpp}} \wedge \left(i_{L_2} < i_{L_1}\right)\right\}$$

$$G^s(T_{21}) = \left\{x \in \frac{\mathrm{x}}{v_{pv}<v_{mpp}} \wedge \left(i_{L_2} = i_{L_1}\right)\right\}$$

$$G^s(T_{13}) = \left\{x \in \frac{\mathrm{X}}{v_{pv} > v_{mpp}} \wedge \left(i_{L_2} > i_{L_1}\right)\right\}$$

$$G^s(T_{31}) = \left\{x \in \frac{\mathrm{X}}{v_{pv} < v_{mpp}} \wedge \left(i_{L_2} = i_{L_1}\right)\right\}$$

In the following, we design an algorithm called Hybrid Maximum Power Point Tracking. The overall flow chart of HMPPT is shown in Figure 4.

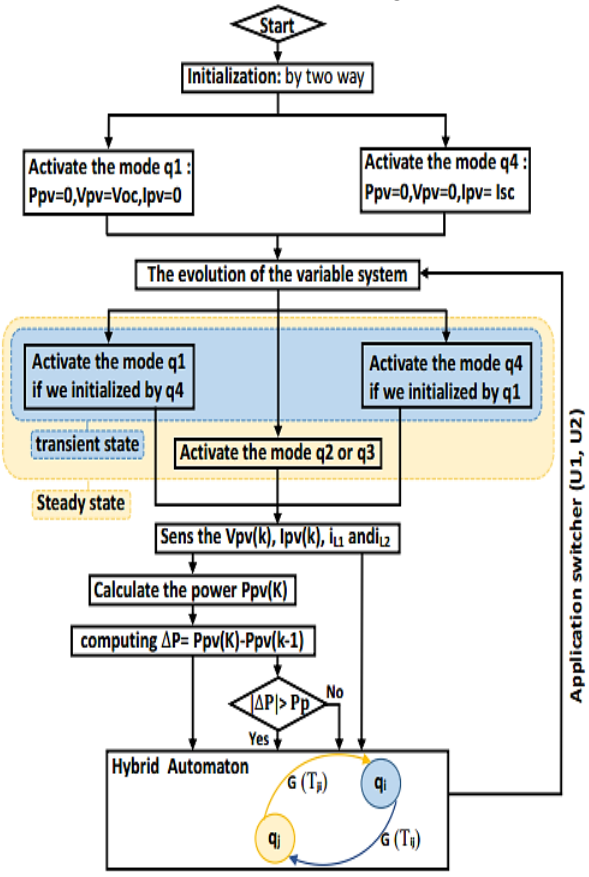

Figure 4. Flow chart of HMPPT

The algorithm itself is straightforward, the constants and variables of this algorithm, namely the voltage, input current, power are initialized.

By using the actual value of voltage and current of the PV array, we calculate the power and compare it with the previous value.

If the difference is positive between them and it is greater than the constant value P_p, then we

increase the voltage by the discharge of both inductances.

If the difference is negative between them and it is greater than the constant value P_p, then the voltage is decreased by charging one of the inductors or both (case of q_4).

We can summarize this stage under the name of transition state. Furthermore, if the difference between them is less than the constant value P_p, meaning that the voltage reaches a neighbourhood of MPP, this stage is called the steady state. The constant value P_p is choosing wisely, so we do not take a large value to avoid the loss of accuracy, and do not take a zero value to avoid the increase number of switching around maximum power point by searching the exact MPP that will delay the balancing of the converter floating currents. This value is related to the photovoltaic array size.

Note 1. We can delete the mode (q_4) from the proposed control because the algorithm does not pass in this situation, so we satisfied with switching between the two modes (q_2 and q_3) according to the amount of the two currents. This occurs when the operating point is to the right of the maximum point, and we can see to what degree it will simplify this algorithm.

4. Simulation Results

In this section, the new hybrid algorithm is applied to a typical converter where the photovoltaic array is used to charge a battery. The performance and robustness of the hybrid algorithm will be tested through different scenarios of irradiance and temperature.

For the battery, we consider an example of 100 Ah lead acid battery with the nominal current discharge characteristic at 0.2C (20A) shown in Table 2.

Table 2. Lead acid battery discharge characteristic

Nominal current discharge characteristic at 0.2C (20A)						
Voltage(v)	12.9	12.1	12	11	9	0
Time(hours)	0	0.05	2	4	5	5.5

The parameters of the battery and the PV module are shown in Table 3.

Table 3. The specifications of the model for the overall PV system in the MATLAB simulation

Model parameters	Value of parameters	Tools modelling
Specifications of the PV module:		Simscape
Short circuit current (I_{SC})	5.2 [A]	
Open circuit voltage (V_{OC})	22 [V]	
Current at Pmax (I_{MPP})	4.77 [A]	
Voltage at Pmax (V_{MPP})	17.9 [V]	
Maximum power (P_{MPP})	85.383 [W]	
V_{OC} coef. of temperature (K_V)	-0.34 [V/°C]	
I_{SC} coef. of temperature (K_I)	0.034 [A/^{0}C]	
N. Cells per module (Ncell)	36	
Specifications for the interleaved buck converter:		Simscape
Input capacitor (C_{in})	900 [µF]	
Output capacitor (C_o)	1000 [µF]	
Inductors ($L_1 = L_2 = L$)	1 [mH]	
Specifications of the Battery:		Simscape
Nominal voltage	12 [V]	
Rated capacity	100 [Ah]	
Initial state of charge	50 [%]	

The PV array consists of 2 parallel strings with 2 series-connected modules per string.

The temperature and the state-of-charge are factors that influence the charging of the battery, but the irradiance is the major factor that affects this process seriously.

To study the performance of the hybrid algorithm under the gradual irradiance changes, two popular MPPT techniques, Incremental Conductance (IC), Perturb and Observe (P&O conventional) can be compared. Gradual change of the irradiance (Table 4) presents the irradiance profile, in which the irradiance is increased in ramp within just 0.5 second.

Table 4. The gradual change of irradiance profile

Irradiance(KW/m^2)	Time(s)
600	[0-0.05]
650	[0.1-0.15]
750	[0.2-0.25]
850	[0.3-0.35]
1000	[0.4-0. 5]

A comparison of the MPP tracking between three algorithms P&O, IC and the hybrid algorithm is performed when they are subjected to this profile; this is illustrated in Figure 5.

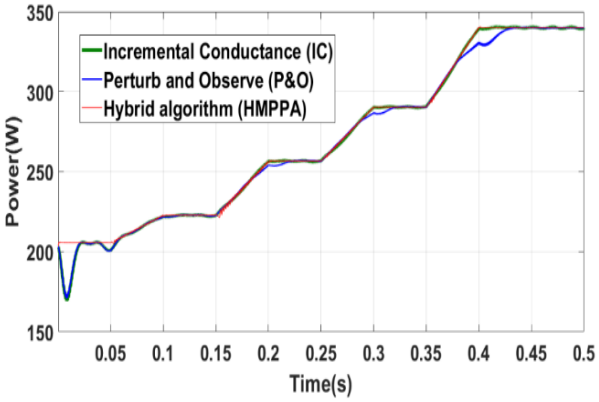

Figure 5. Response of three algorithms (IC, P&O, HMPPA) under gradual change of the irradiance

The initial parameter value of the two algorithms P&O and IC are chosen after extensive simulation trials, so we would say that the algorithms could be regarded as well optimized. For P&O, a fixed step size of 1 V is chosen in order to increase/decrease the duty cycle D (the increase in v_{ref} means the decrease in D), this value should be selected carefully in order to achieve a balance between the convergence speed and the oscillation in the steady state. For IC, the maximum error $\frac{dI}{dV}$ can be defined as constant error E = 0.002, this technique is based on the variation of conductance and their effect on the position of the operating point.

Initially, both P&O and IC require approximately 0.022 s to reach the MPP.

When the steady state is reached, the two algorithms fluctuate around the maximum power point. On the other hand, the hybrid algorithm has a very good performance in terms of fast tracking to the maximum power point in the transient state with almost zero power oscillation in the steady state.

When the irradiance changes in gradual (ramp in the profile), the P&O track badly the power compared to its counterpart IC. Both, however, could not track the power ramp as perfectly as the hybrid algorithm does, which means that the P&O and IC loses the power during tracking the power ramp and this is clearly shown in Figure 5.

Step changes of the irradiance, this change usually occurs when a cloud passes quickly. To examine the performance of the hybrid algorithm, a PV array is subjected to a set of radiation steps, as shown in Figure 6 and Table 6.

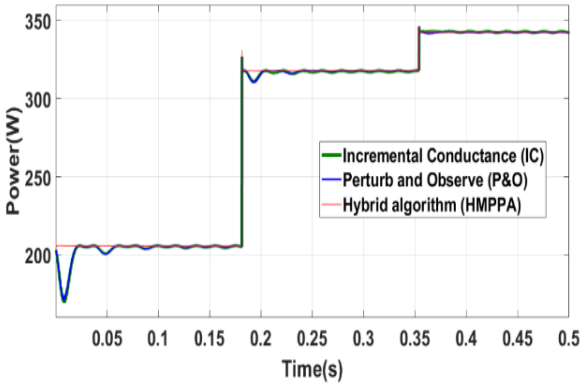

Figure 6. Response of three algorithms (IC, P&O, HMPPA) under step change of the irradiance

Table 6. The step change of irradiance profile

Irradiance (KW/m^2)	Time (s)
600	[0-0.18]
920	[0.18-0.35]
1010	[0.35-0.5]

In this test, the temperature is considered constant at 25 °C.

Figure 6 compares the response of the three algorithms (P&O, IC and HMPP). The P&O and IC have almost the same response with a small difference, whereas the IC is a little better than the P&O in terms of transit state, which requires 22.5 ms for the initial MPP tracking. The small step-size can be selected to reduce the large oscillation around the MPP. From Figure 6, it can be observed that even with a small step-size, P&O oscillates around the MPP with a ripple of 2 W, while the ripple in the HMPP is almost negligible (0.03 W). After each change of irradiance level, the P&O requires approximately 21 ms to re-track the new MPP value, while the HMPP needs only 2 µs.

The reason that lies behind the speed of response for the algorithm is the number of commutations between the discrete states, indeed; only one commutation can be applied to reach the steady state. The ripple of the PV current and the PV voltage is very small and almost non-existent.

The battery current is charging, and the voltage is imposed by the battery. The current and voltage levels of the battery depend on the battery system conditions such as the state-of-charge.

The battery has a protection system, which will stop the system if the SOC goes under SOC_{min} or when the SOC exceeds SOC_{max}.

5. Conclusions and Future Works

This paper proposes a novel hybrid algorithm for maximum power point tracking (HMPPT). This control applies to a particulary topology of converters, which is the 2-phases interleaved buck converter, this choice is motivated by the interesting practical benefits compared to standard ones.

In this study, we used a hybrid dynamical approach to design the control of the photovoltaic system via a hybrid automaton formalism to control the transition between the different modes, and this is done by choosing the appropriate guard conditions.

The obtained simulations results confirm the proposed hybrid algorithm (HMPPT) such as the fast transient and less fluctuation at the MPP.

As a future work, a generalization of the proposed hybrid controller to N-phases interleaved buck converter and other multilevel topologies will be considered. We explore the subject matter with a complete study of the system including the battery, the micro-grid and maybe with multiple sources like a fuel cell. Hence, an experimental validation will be provided.

6. Bibliographic References

[1] Lupangu C., Bansal R., A review of technical issues on the development of solar photovoltaic systems, Renewable and Sustainable Energy Reviews 73 (2017) pp. 950–965.

[2] Jamal T., Urmee T., Calais M., Shafiullah G., Carter C., Technical challenges of {PV} deployment into remote australian electricity networks: A review, Renewable and Sustainable Energy Reviews (2017).

[3] Balogh L., Redl R., Power-factor correction with interleaved boost converters in continuous inductor-current mode, in: Applied Power Electronics Conference and Exposition, 1993. APEC'93. Conference Proceedings 1993, Eighth Annual, IEEE, 1993, pp. 168–174.

[4] Subramanian N., Prasanth P., Srinivasan R., Subesh R., Seyezhai R., A comparative study of conventional, coupled inductor and rcn based interleaved boost converter for photo-voltaic applications, in: IET Chennai Fourth International Conference on Sustainable Energy and Intelligent Systems (SEISCON 2013), 2013, pp. 71–77.

[5] Xu H., Qiao E., Guo X., Wen X., Kong L., Analysis and design of high power interleaved boost converters for fuel cell distributed generation system, in: Power Electronics Specialists Conference, 2005. PESC'05. IEEE 36th, IEEE, 2005, pp. 140–145.

[6] Guilbert D., Gaillard A., N'Diaye A., Djerdir A., Power switch failures tolerance and remedial strategies of a 4-leg floating interleaved dc/dc boost converter for photovoltaic/fuel cell applications, Renewable Energy 90 (2016) pp. 14 – 27.

[7] Benmiloud M., Benalia A., Djemai M., Hybrid sliding mode control for two cells converter, in: 2014 13th International Workshop on Variable Structure Systems (VSS), 2014, pp. 1–6.

[8] Middlebrook R., Cuk S., A general unified approach to modelling switching-converter power stages, in: Power Electronics Specialists Conference, 1976 IEEE, pp. 18–34.

[9] Senesky M., Eirea G., Koo T. J., Hybrid modelling and control of power electronics, in: International Workshop on Hybrid Systems: Computation and Control, Springer, 2003, pp. 450–465.

[10] Bougrine M., Benmiloud M., Benalia A., Benbouzid M., Delaleau E., Hybrid control of a two interleaved dc-dc converter for dc bus regulation, in: IECON 2016 - 42nd Annual Conference of the IEEE Industrial Electronics Society, 2016, pp. 3419–3424.

[11] Wen H., Su B., Hybrid-mode interleaved boost converter design for fuel cell electric vehicles, Energy Conversion and Management 122 (2016) pp. 477 – 487.

[12] Barry B. C., Hayes J. G., Ry lko M. S., Ccm and dcm operation of the interleaved two-phase boost converter with discrete and coupled inductors, IEEE Transactions on Power Electronics 30 (12) (2015) pp. 6551–6567.

[13] Sun J., Mitchell D. M., Greuel M. F., Krein P. T., Bass R. M., Averaged modeling of pwm con verters operating in discontinuous conduction mode, IEEE Transactions on Power Electronics 16 (4) (2001) pp. 482–492.

[14] Ouoba D., Fakkar A., Kouari Y. E., Dkhichi F., Oukarfi B., An improved maximum power point tracking method for a photovoltaic system, Optical Materials 56 (Supplement C) (2016) pp. 100 – 106, advanced Materials for Optics, Photonics, Renewable Energies and Their Recent Advances.

[15] Villalva M. G., Ruppert E., Analysis and simulation of the p&o mppt algorithm using a lin earized pv array model, in: Industrial Electronics, 2009. IECON'09. 35th Annual Conference of IEEE, pp. 231–236.

[16] Sivakumar P., Kader A. A., Kaliavaradhan Y., Arutchelvi M., Analysis and enhancement of pv efficiency with incremental conductance mppt technique under non-linear loading conditions, Renewable Energy 81 (2015), pp. 543–550.

[17] Zakzouk N. E., Elsaharty M. A., Abdelsalam A. K., Helal A. A., Williams B. W., Improved performance low-cost incremental conductance pv mppt technique, IET Renewable Power Generation 10 (4) (2016), pp. 561–574.

[18] Alajmi B. N., Ahmed K. H., Finney S. J., Williams B. W., Fuzzy-logic-control approach of a modified hill-climbing method for maximum power point in microgrid standalone photovoltaic system, IEEE transactions on power electronics 26 (4) (2011), pp. 1022–1030.

[19] Azab M., A new maximum power point tracking for photovoltaic systems, WASET. ORG 34 (2008), pp. 571–574.

[20] Casadei D., Grandi G., Rossi C., Single-phase single-stage photovoltaic generation system based on a ripple correlation control maximum power point tracking, IEEE Transactions on Energy Conversion 21 (2) (2006), pp. 562–568.

[21] Ameur K., Ait-Cheikh M. S., Essounbouli N., et al., A pso-based optimization of a fuzzy based mppt controller for a photovoltaic pumping system used for irrigation of greenhouses, Iranian Journal of Fuzzy Systems 13 (3) (2016), pp. 1–18.

[22] Fannakh M., Elhafyani M. L., Zouggar S., Hardware implementation of the fuzzy logic mppt in an arduino card using a simulink support package for pv application, IET Renewable Power Generation.

[23] Larbes C., Cheikh S. A., Obeidi T., Zerguerras A., Genetic algorithms optimized fuzzy logic control for the maximum power point tracking in photovoltaic system, Renewable Energy 34 (10) (2009), pp. 2093 – 2100.

[24] Jiang L. L., Maskell D. L., Patra J. C., A novel ant colony optimization-based maximum power point tracking for photovoltaic systems under partially shaded conditions, Energy and Buildings 58 (Supplement C) (2013), pp. 227 – 236.

[25] Punitha K., Devaraj D., Sakthivel S., Artificial neural network based modified increment tal conductance algorithm for maximum power point tracking in photovoltaic system under partial shading conditions, Energy 62 (Supplement C) (2013), pp. 330 – 340.

[26] Benmiloud M., Contribution to the Analysis and Control Design of Hybrid Dynamical Systems Application to Multicellular Converters, University of Amar Telidji, Laghouat-ALGERIA, 2017.

[27] Haddadi K., Gazzam N., Benalia A., "Algebraic observer design for switched linear systems applied to multicellular converters for estimating capacitor voltages", in Electrotehnica, Electronica, Automatica (EEA), 2017, vol. 67, no. 1, pp. 28-34, ISSN 1582-5175.

[28] Ameur I., Gazzam N., enmiloud M., Benalia A., "Output Feedback Control of Multicellular Converters" International Journal of Dynamics and Control, 2019.

[29] Lunze J., Lamnabhi-Lagarrigue F., Handbook of hybrid systems control: theory, tools, applications, Cambridge University Press, 2009.

Funding Sources

This work was financially supported by the LACoSERE Laboratery. University Amar Telidji of Laghouat, Algeria.

Authors' Biographies

Iyad Ameur was born on 16 August 1988 in Laghouat/Algeria.
He earned his License degree in Electro-technology (2010) and his Master degree in Automatic (2012) from the Amar Telidji university, Laghouat.
He is a PhD Student in the Electrical Engineering Department. His general research interests are in the areas of Automatic control systems and his current research focuses on the control of hybrid dynamical systems (switched linear systems- DC/AC converters) as well as photovoltaic systems.
e-mail: iy.ameur@lagh-univ.dz

Mohammed Benmiloud was born on 13 December 1988 in Laghouat/Algeria.
He earned his License degree in Electro-technology (2009) and his Master degree in Automatic (2011) from the Amar Telidji university, Laghouat.
He is currently a PhD Student in the Electrical Engineering Department. His general research interests are in the areas of Automatic control systems and his current research focuses on the control of hybrid dynamical systems. Now, he is working in "Research Associate in the Analysis and Control of Large Scale Networks" at the university of Cambridge.
e-mail: med.benmiloud@lagh-univ.dz

Atallah BENALIA was born on 1972 in Algiers/ Algeria. He received the diploma of state engineer from Ecole Polytechnique of Algiers in 1996, and the DEA and PhD degrees in Automatic control from the University of Paris-Sud (France), in 1998 and 2004, respectively.
He joined the faculty of the Technology at the University of Amar Telidji, Laghouat (Algeria), in 2008 where he is currently a professor. His research interests deal mainly with analysis and control of nonlinear systems.
e-mail: a.benalia@lagh-univ.dz